HHS Public Access

Author manuscript

Br J Dermatol. Author manuscript; available in PMC 2018 July 01.

Published in final edited form as:

Br J Dermatol. 2017 July ; 177(1): 168–178. doi:10.1111/bjd.15236.

miR-203 and *miR-205* expression patterns identify subgroups of prognosis in cutaneous squamous cell carcinoma

J. Cañueto[1,2], **E Cardeñoso-Álvarez**[3,#], **J.L. García-Hernández**[2,4,#], **P. Galindo-Villardón**[5], **P. Vicente-Galindo**[5], **J.L. Vicente-Villardón**[5], **D. Alonso-López**[2,4,6], **J. De Las Rivas**[2,4,6], **J. Valero**[4], **E. Moyano-Sanz**[1], **E. Fernández-López**[1,2], **J.H. Mao**[7], **A. Castellanos-Martín**[2,4,¶,*], **C. Román-Curto**[1,2,*], and **J. Pérez-Losada**[2,4,*]

[1]Departamento de Dermatología. Hospital Universitario de Salamanca. Paseo de San Vicente, 58-182, 37007. Salamanca. Spain

[2]Instituto de Investigación Biomédica de Salamanca (IBSAL). Hospital Universitario de Salamanca. Paseo de San Vicente, 58-182, 37007. Salamanca. Spain

[3]Departamento de Dermatología. Hospital Virgen de la Concha. Avenida de Requejo. Zamora. Spain

[4]Instituto de Biología Molecular y Celular del Cáncer (IBMCC). Centro de Investigación del Cáncer (CIC). Universidad de Salamanca/CSIC. Campus Miguel de Unamuno, s.n. 37007. Salamanca. Spain

[5]Departamento de Estadística. Universidad de Salamanca. Campus Miguel de Unamuno, s.n. 37007. Salamanca. Spain

[6]Unidad de Bioinformática, CIC-IBMCC. Salamanca, 37007. Spain

[7]Life Sciences Division, Lawrence Berkeley National Laboratory, University of California, Berkeley, CA 94720. Lawrence Berkeley National Laboratory (LBNL). Berkeley. CA. USA

Abstract

Cutaneous squamous cell carcinoma is the second most widespread cancer in humans and its incidence is rising. These tumours can evolve as poor-prognosis diseases, and therefore it is important to identify new markers to better predict its clinical evolution. Here, we identified the expression pattern of miRNAs at different stages of skin cancer progression in a panel of murine skin cancer cell lines. We determined that *miR-203* and *miR-205* are differentially expressed in this panel, and evaluated their potential use as biomarkers of prognosis in human tumours. *MiR-205* was expressed in tumours with pathological features recognized as indicators of poor prognosis such as desmoplasia, perineural invasion and infiltrative growth pattern. *MiR-205* was mainly expressed in undifferentiated areas and in the invasion front, and was associated with both local recurrence and the development of general clinical events of poor evolution. *MiR-205*

Corresponding authors: Javier Cañueto (jcanueto@yahoo.es) and Jesús Pérez-Losada (jperezlosada@usal.es).
[#]These authors contributed equally as second authors.
[*]These authors contributed equally as senior authors.
[¶]*Current address: Institute for Research in Biomedicine (IRB). Barcelona. Spain.*

COMPETING INTERESTS

The authors state no conflict of interest.

expression was an independent variable selected to predict events of poor clinical evolution using the multinomial logistic regression model described in this study. In contrast, *miR-203* was mainly expressed in tumours exhibiting the characteristics associated with a good prognosis, was mainly present in well-differentiated zones, and rarely expressed in the invasion front. Therefore, the expression and associations of *miR-205* and *miR-203* were mostly mutually exclusive. Finally, using a logistic biplot we identified three clusters of patients with differential prognosis based on *miR-203* and *miR-205* expression, and pathological tumour features. This work highlights the utility of *miR-205* and *miR-203* as prognostic markers in cutaneous squamous cell carcinoma.

Keywords

Cutaneous Squamous Cell Carcinoma; miRNAs; *miR-205*; *miR-203*; P63; E-CADHERIN; Prognosis

INTRODUCTION

Cutaneous squamous cell carcinoma (CSCC) is the second most common cancer in humans after basal cell carcinoma [1, 2]. The incidence of CSCC is rising dramatically. It is estimated that more than 700,000 new CSCC cases are diagnosed in the US per year [3], leading to high health care costs [4]. The risk of developing CSCC along human life is between 7% and 11% [5]. The incidence of CSCC varies in different geographical areas and countries [6]. Owing to the high frequency of CSCC, it is the non-melanoma skin cancer that causes most metastases and deaths [3].

CSCC can evolve as a poor-prognosis disease. Although significant advances have been made in our understanding of the development of CSCC, there are many unknown aspects concerning its pathogenesis and prognosis. Thus, it is necessary to seek molecular markers that can help physicians to predict the biological behaviour and clinical evolution of CSCC. Recently, microRNAs (miRNAs or miRs) have emerged as a new class of molecules closely related to the pathogenesis of cancer [7]. MiRNAs are small molecules of non-codifying RNA of 17–25 nucleotides that act as posttranscriptional regulators of mRNA expression [8]. MiRNAs have been implicated in the pathogenesis of several forms of cancer [7], and their expression patterns may have prognostic value [9–11].

Despite the fact that important work has been done regarding the role of miRNAs in the Biology of CSCC [12, 13], and other skin cancers, such as basal cell carcinomas [14], the utility of miRNAs in defining the prognosis of the disease still requires further study. Although some authors have evaluated the expression patterns of miRNAs in skin cancer cell lines [15] and in CSCC [16], their potential prognostic value has not been explored in detail. In the present work, we identified differential miRNA expression patterns along different stages of CSCC progression in a well-established panel of murine skin cancer cell lines [17–20]. Later, based on our findings and previous data in the literature, we selected *miR-205* and *miR-203* to evaluate their association with the clinical prognosis and evolution of human CSCC [21–27]. Based on the expression of *miR-203* and *miR-205* and pathological tumour features, we predicted the prognosis of CSCC using multinomial logistic regression models. We also

identified three clusters of CSCC with a logistic biplot, which highlights the utility of *miR-203* and *miR-205* expression to predict CSCC prognosis.

PATIENTS, MATERIAL AND METHODS

Patients and tumour variables

Seventy-nine human primary CSCCs were collected at the University Hospital of Salamanca in Spain. The collection and use of tumour samples were approved by the institutional Ethics Review Board of the University Hospital of Salamanca. Written informed consents for research using these tumour samples were obtained from all patients. We evaluated different pathological and clinical variables of evolution whose distribution is described on Supplementary Table S1.

Cell lines

We used a panel of murine cell lines that represent different stages of CSCC, a generous gift from Dr. Balmain (USCF). The panel includes (i) non-tumoural cell lines: C50, C5N; NK; (ii) papilloma cell lines: MSCP1 and P6; (iii) malignant, well-differentiated cell lines with squamous morphology: PDV, PDVC57, B9 and E4; and, (iv) poorly-differentiated cell lines, with the epithelial to mesenchymal transition (EMT) phenotype: H11, D3, A5, CarB and CarC [17–20]. Cells were cultured in DMEM supplemented with 10% foetal bovine serum (FBS), 1% penicillin-streptomycin and 4 mM L-glutamine at 37°C and 5% of CO_2.

Total RNA isolation

Cells were collected and centrifuged at 1500 r.p.m. Total RNAs were isolated using the Qiagen™ kit (miRNA easy) following the manufacturer's instructions. Briefly, RNAs were extracted with a mix of phenol-chloroform followed by precipitation in ethanol, and were purified through RNase-free columns. RNA concentrations were determined with a spectrophotometer (Nanodrop) and microfluidic chips (Agilent).

miRNA expression analysis

MiRNA expression was analysed with specific arrays miRCURY LNA microRNA Array, v. 10.0 (Exiqon), following the manufacturer's recommendations. Then, fluorescent reagents were reconstituted and cDNAs were synthesized and labelled. Following this, samples were heated at 95° C in darkness, hybridized, and washed with the robotic HS 4800 Pro system (Tecan®). Fluorescence was scanned with a GenePix 4000B (Axon Instruments™) microarray scanner. Image processing was accomplished with the Gene Prix Pro (v 6.0). The data for the analysis were generated from a single channel following manufacturer's instructions. Raw data processing was performed with the ExiMiR package from R [28, 29]. Quantile normalization was performed using the Robust Microarray Analysis (RMA) algorithm[30] from the BioConductor (http://www.bioconductor.org/) tools suite. All expression data were deposited in the GEO database (GEO: GSE71923).

Tissue-array and *in situ* hybridization

Tissue samples embedded in paraffin were used to prepare tissue microarrays with a tissue arrayer device (Beecher Instruments, MD). Three 1-mm diameter tissue cylinders from each tumour were included. Different areas of each tumour were selected to analyse the heterogeneity of tumours. *MiR-203* and *miR-205* expression was detected in the tissue sections by *in situ* hybridization (ISH) using the *miRCURY LNA™ microRNA ISH kit* (Exiqon®) and following the manufacturer's recommendations.

For the quantification of miRNA expression, we evaluated the percentage of positive cells, the intensity of the staining and the location as follows: the intensity of staining was considered negative when there were no stained cells or there were fewer than 5% of stained cells; weakly positive (+) when the percentage of stained cells was more than 5% and less than 25%; moderately positive (++) when more than 25% and less than 75%; intensely positive (+++) when more than 75% of the cells were stained. Analysis of miRNA expression by ISH was performed by three independent observers (J.C., C.R.C and E.C.A).

Immunohistochemistry

P63 and E-CADHERIN expressions were evaluated by immunohistochemistry with specific antibodies against P63 (Biocare, Clon BC4A4) and E-CADHERIN (Vitro, Clone EP700Y). We evaluated P63 and E-CADHERIN expression with the same semiquantitative method as that used to assess miRNA expression, described in the Supplementary Materials and Methods section.

Statistical analyses

To compare dichotomous variables we used the Chi-square or the Fisher exact tests, and to evaluate two independent samples, the Mann-Whitney U test. To assess more than two independent groups we used the Kruskal-Wallis test. To compare temporal intervals we used the Kaplan-Meier estimator, followed by the Mantel-Cox Log-Rank test. To build graphical representations of the statistical associations among variables, we used the Cytoscape (v. 3.1.0) software, freely available at www.cytoscape.org (accessed December 11th 2014). To evaluate which variables predicted events of poor clinical evolution, we developed logistic regression models and used the Wald test. We considered P values < 0.05 as significant, and confidence intervals at 95%. To generate clusters of prognosis we used the logistic biplot [31].

RESULTS

Tumours with poor clinical evolution are associated with specific histopathological traits

We defined CSCCs with poor clinical evolution as those tumours that presented local recurrence, lymph nodal progression or metastases to distant organs. In the literature, a number of other types of histopathological tumour traits associated with poor clinical evolution of CSCC have been established, such as poor degree of differentiation, perineural infiltration, infiltrative growth pattern, desmoplasia, etc. [32–34]. Therefore, we first evaluated to what extent the tumours in our cohort, known to have a poor clinical outcome, exhibited these histopathologic features, all associated with a poor prognosis (Table 1A). Undoubtedly, perineural infiltration was statistically more frequent in tumours with local recurrence (P =

0.002) and with lymph nodal progression ($P = 0.048$). Thicker tumours also showed more local recurrence ($P = 0.009$) and lymph nodal progression ($P = 0.035$). Nodal progression was also associated with a poor grade of differentiation ($P = 0.006$) (Table 1A). We did not find statistical association with dissemination to distant organs because of the low number of tumours with this clinical event (N = 1) in our series (Supplementary Table S1). As expected, we observed several associations among the different histopathological tumour traits, which in turn were also associated with poor or good prognosis based on the literature (Supplementary Table S2). In conclusion, in our cohort of CSCC we observed a number of associations among several pathological tumour traits with events of poor clinical evolution.

Identification of miRNA differentially expressed in skin cancer cell lines with different grade of aggressiveness

Owing to the increasing importance of miRNAs in the pathogenesis of cancer [9–11], we considered the possibility that miRNAs could help to define the prognosis of CSCC. To identify miRNAs that could be associated with human CSCC with different grades of aggressiveness and prognosis, we identified miRNAs differentially expressed between groups of CSCC cell lines. Later, we chose some of these miRNAs to be evaluated in human CSCC prognosis, because of their importance in skin homeostasis.

As a result, we identified a number of miRNAs overexpressed in squamous non-malignant cell lines (C5N, NK, MSCP1, P6) when compared to a group of malignant cell lines with a squamous morphology (PCVC57, B9, E4) (Figure 1A and Supplementary Table S3A). Among the miRNAs most differentially expressed in the immortalized non-malignant group, we identified some miRNAs already known as tumour suppressors within different contexts, such as *let-7, miR-34b, miR-200c*, others with protumoural effects, such as *miR-19a* [35, 36], and others related to skin homeostasis, such as *miR-203* and *miR-205* [14, 21, 23, 37, 38] (Figure 1A and Supplementary Table S3A). We also identified miRNAs downregulated in the EMT stage, within squamous CSCC cell lines (PCVC57, B9, E4) compared to spindle CSCC cell lines (D3, H11, CarB, CarC, A5). In our study, the miRNA most differentially expressed was *miR-205*, which is in agreement with the fact that it can inhibit EMT in CSCC [39] (Figure 1B and Supplementary Table S3B).

Because of the importance of *miR-203* and *miR-205* in skin homeostasis, we initially focused on these two miRNAs [14, 21, 23, 37, 38]. It was observed that *miR-205* was more expressed in non-malignant and squamous CSCC cell lines than in spindle CSCC cells ($P = 0.041$). In contrast, *miR-203* was more expressed in squamous non-malignant cell lines than in the malignant groups with a statistical trend ($P = 0.086$) (Figure 1C).

Mutually exclusive expression patterns of *miR-203* and *miR-205* in CSCC

Next, we evaluated the expression of *miR-203* and *miR-205* in human CSCCs. First, we confirmed the expression patterns of both miRNAs in the normal adjacent skin, as described within the literature. Thus, *miR-203* was predominantly expressed in the upper layers of the skin [40], and *miR-205* was mostly expressed in the basal and immediate suprabasal layers [41] (Figure 2A).

We then evaluated the expression patterns of *miR-205* and *miR-203* in CSCC and found them to be reciprocally exclusive (Figure 2B and Supplementary Table S4). *MiR-203* was more frequently expressed, to a moderate or intense degree, in differentiated rather than in undifferentiated areas ($P = 0.014$), whereas *miR-205* was more frequently expressed at high levels in undifferentiated areas ($P < 0.0001$) in the invasion front ($P = 0.0008$) and in zones with perineural invasion (Figures 2C–F, and Supplementary Table S4). Interestingly, we observed that tumour cells, inside a blood vessel and forming a thrombus, sometimes overexpressed *miR-205* (Figure 2F).

In addition, *miR-205* was, in general, more frequently expressed in tumours with an infiltrative growth pattern ($P = 0.003$), perineural invasion ($P = 0.016$), and in thicker tumours ($P = 0.023$) - all pathological tumour traits associated with a poor prognosis [32, 33, 42]. By contrast, *miR-203* expression was not associated with these same tumour traits (Supplementary Table S5A).

Regarding the expression of these miRNAs in the invasion front, it was determined that *miR-205 was* more frequently expressed in tumours with aggressive traits, such as infiltrative growth pattern and perineural invasion. However, *miR-203* was significantly less expressed in the invasion front of such aggressive tumours (Supplementary Table S5B). In conclusion, *miR-205* and *miR-203* tended to exhibit mutually exclusive expression patterns in human CSCC.

Reciprocally exclusive associations between *miR-205* and *miR-203* and P63

It has been reported that *miR-203* inhibits P63, leading to cell differentiation and the repression of stemness [21, 23], whereas *miR-205* represses E-CADHERIN and expands into the stem cell compartment [41]. Thus, we evaluated the associations of *miR-203* and *miR-205* with P63 and E-CADHERIN as grading markers in epithelial differentiation. As expected, P63 was more frequently expressed in poorly differentiated tumours, and it was significantly more common in undifferentiated areas, whereas E-CADHERIN expression was more intense in well-differentiated tumours, and less common in undifferentiated areas (Figures 2C, 2D and 2G).

P63 was inversely correlated to *miR-203* expression, and most of the tumours with a remarkable P63 expression did not show *miR-203* ($P = 0.009$). Conversely, the majority of tumours with P63 expression showed expression of *miR-205* ($P = 0.0001$). We did not observe a statistically significant association between the expressions of *miR-205* and E-CADHERIN in the tumours of our cohort (Figure 2H and Supplementary Table S5C). In conclusion, *miR-203* and *miR-205* showed a mutually exclusive P63 protein distribution in human CSCC.

Prediction of CSCC prognosis based on miRNAs expression and tumour traits

We later evaluated the association between events of poor prognosis and *miR-205* and *miR-203* expression. *MiR-205* expression was associated with local CSCC recurrence ($P = 0.038$), and with the general events related to a poor clinical evolution ($P = 0.011$). We could not find an association between the expression of *miR-203* with specific events of poor prognosis (Table 1B).

To predict the prognosis of CSCC, we built a logistic regression model in order to predict local recurrence, lymph nodal progression, and the existence of any event associated with a poor clinical evolution. As predictive variables, we used *miR-203* and *miR-205* expression, perineural invasion, the grade of differentiation (well-differentiated *versus* poorly-moderately differentiated), the growth pattern of invasion (infiltrative *versus* non-infiltrative), tumour thickness (more than 2 mm *versus* less than 2 mm), and tumour surface size (more than 20 mm *versus* less than 20 mm in the largest diameter).

Perineural invasion was the only independent variable associated with local recurrence ($P = 0.017$); and a low grade of differentiation was the only variable related to lymph nodal progression ($P = 0.004$). Interestingly, *miR-205* expression was the only independent variable associated with the occurrence of any general outcome of poor clinical evolution ($P = 0.021$) (Table 2A). In summary, here we report that the logistic regression models are capable of predicting the clinical evolution of CSCC, based on miRNA expression and the pathological features of tumours.

Identification of clusters of human CSCC with different prognoses

We then attempted to sort the 79 CSCCs from our study into clusters of different prognoses based on the multiple associations among the tumour traits and the expression of *miR-203* and *miR-205* using a logistic biplot [31]. Thus, we included pathological variables involved in the prognosis of CSCC such as: the presence/absence of perineural invasion and desmoplasia, the degree of differentiation, the growth pattern of invasion, the tumour size and thickness [32, 34, 43], together with the expression of *miR-203* and *miR-205*. We were able to discriminate three clusters of tumours, with different prognoses and with statistically significant differences, using all of the tumour characteristics considered (Table 2B and Supplementary Figure S1).

Cluster 1 comprised 25 CSCCs (31.6%), but only one developed a clinical outcome of poor prognosis. In this cluster, only three tumours (12%) showed *miR-205* expression, but 15 (60%) expressed *miR-203*. In addition, this cluster contained several tumours with pathological traits of a good prognosis. In addition, there was only 1 tumour with perineural infiltration, 1 tumour with desmoplasia and 2 tumours with a poor grade of differentiation.

At the far end of cluster 1, cluster 3 comprised 23 CSCCs (29.1%) with the characteristics of a poor prognosis, and 8 tumours (34.8%) developed outcomes of poor clinical evolution. Interestingly, 21 (91.3%) tumours expressed *miR-205*, and only 3 (15%) expressed *miR-203*. This cluster contained several tumours with histopathological traits of poor prognosis; in addition, 22 (95%) showed an infiltrative growth pattern, 13 (56.5%), a poor grade of differentiation, and the same percentage of tumours with perineural infiltration and desmoplasia (Table 2B and Supplementary Figure S1).

In total, all clusters were well characterized by the percentage of tumours that expressed *miR-205* and *miR-203*; such that a progressively increasing expression of *miR-205* went from 12% of tumours in cluster 1 to 91% of tumours in cluster 4; whereas the trend of *miR-203* expression was the opposite. This perfectly correlated with the percentage of cases with poor clinical evolution in each clusters, although the pathological tumour traits,

including infiltrative growth pattern and poor grade of differentiation, showed a worse correlation among all three clusters (Table 2B and Supplementary Figure S1). Thus, although this study requires further validation using a new cohort of patients, in our cohort, the expression of these two *miRNA*s more accurately sorted tumours in terms of prognosis than the pathological features. In conclusion, this study illustrates the usefulness of *miR-203* and *miR-205* in predicting the prognosis of human CSCC.

DISCUSSION

Here we have evaluated miRNA expression and histopathological tumour features of human CSCC, and its association with local recurrence, lymph node dissemination and metastasis to predict clinical prognosis. *MiR-205* expression in the primary tumour was associated with local recurrence (Tables 1B and 2A). We have also demonstrated the differential localization of *miR-203* and *miR-205* in human CSCC (Figures 2B–E), and have evaluated the associations of the expression pattern of *miR-203* and *miR-205* with pathological traits of CSCC. Overall, *miR-203* and *miR-205* were associated with different tumour traits in a mutually exclusive manner (Supplementary Tables S4 and S5). Thus, *miR-205* was associated with clinical and histopathological variables of poor outcome.

Not much is known about the role *of miR-205* in the pathogenesis of CSCC. It has been pointed out that *miR-205* expression is higher in CSCC than in normal skin [15], in which it is restricted to basal layer progenitors. *MiR-205* maintains epithelial proliferation during the development of skin [41], and the lack of expression of *miR-205* inhibits the proliferation of cells of the basal layer. Although it has been described that *miR-205* inhibits EMT through the inhibition of ZEB factors [39], we observed the expression of *miR-205* in undifferentiated areas, zones of perineural invasion and along the invasion front in CSCC (Figures 2C–F and Supplementary Tables S4 and S5). This could be in agreement with the fact that a pure EMT is rarely observed in the invasion front of epithelial tumours of human origin. In fact, while a complete EMT is accepted as a critical step during embryogenesis, its participation in carcinoma metastasis is debated by several authors [44–46].

Here we observed a statistical association between *miR-205* expression and local recurrence. Moreover, *miR-205* expression was the only independent variable selected by a logistic regression model to define general events of poor evolution of CSCC (Table 2A). These facts, together with the expression of *miR-205* in undifferentiated zones and in the invasion front suggest a protumoural role for *miR-205* in the pathogenesis of CSCC. *MiR-205* would probably help to maintain a poorly differentiated and more aggressive epithelial phenotype in the tumours, but at the same time would be an epithelial marker and would inhibit the whole mesenchymal transformation. It has been described that *miR-205* could activate AKT in normal skin [41] and in carcinomas of other origins [47–49]. This is also consistent with the inverse correlation between *miR-205* and the positive correlation with P63, found in this study, and in agreement with previous works [22, 50, 51]. Recently it was demonstrated that EMT occurs in parallel with AKT activation during CSCC invasion [52].

Despite the important role of *miR-203* in keratinocyte homeostasis [21], its role in CSCC has not been previously studied. Here, we did not find statistical association with events of poor

clinical evolution, but according to our data, *miR-203* helps to identify a subgroup of CSCC with a better prognosis (Table 2B and Supplementary Figure 1). This could be in agreement with the fact that *miR-203*, which has an antitumoural effect in basal cell carcinomas [14], has been observed as being repressed in CSCC in mice [26], and also inhibits epithelial to mesenchymal transition [24]. In conclusion, *miR-203* could behave as a tumour suppressor in human CSCC, but additional studies are needed to clarify this possibility. An interesting aspect was the mutually exclusive pattern of expression between *miR-203* and *miR-205* in tumours, depending on the degree of differentiation, and in the invasion front (Figure 2 and Supplementary Tables S4 and S5).

Finally, we identified three clusters of tumours with different prognoses by integrating the expression pattern of these miRNAs with clinical and pathological parameters. Although these clusters encompassed different pathological variables, they were well defined by the percentage of cases that expressed *miR-203* and *miR-205*, and indeed, *miR-203* and *miR-205* sorted tumours in terms of prognosis more accurately than histopathological variables alone. Thus, these miRNAs could be used as markers of prognosis in CSCC. Finally, taking into account that miRNAs are master molecules that affect different processes in cellular homeostasis through the regulation of multiple proteins, miRNA-based targeted therapies might be more effective than those directed towards a single protein. Accordingly, they may become interesting potential therapeutic targets in CSCC.

Supplementary Material

Refer to Web version on PubMed Central for supplementary material.

Acknowledgments

We thank Dr. Balmain for the panel of skin cancer cell lines. JPL was partially supported by FEDER and MICINN (PLE2009-119, SAF2014-56989-R), Instituto de Salud Carlos III (PI07/0057, PI10/00328, PIE14/00066), Junta de Castilla y León (SA078A09, CSI034U13, CSI001U16), the “Eugenio Rodríguez Pascual”, the “Fundación Inbiomed” (Instituto Oncológico Obra Social de la Caja Guipozcoa-San Sebastian, Kutxa), IBSAL (IBY15/00003), and the “Fundación Sandra Ibarra de Solidaridad frente al Cáncer”. C R-C is funded by Q3718001E (2009-2010) y GRS 612/A/11 (2011-2012) and “the Fundación Eugenio Rodríguez Pascual”. AC was supported by FIS (PI07/0057) and MICINN (PLE2009-119). JHM was supported by the National Institutes of Health, a National Cancer Institute grant (R01 CA116481), and the Low-Dose Scientific Focus Area, Office of Biological & Environmental Research, US Department of Energy (DE-AC02-05CH11231). We thank Dr. Sánchez-García for useful comments of the manuscript and Nicholas Skinner and Emma Keck from the University of Salamanca for their help in English editing. We apologize to the many colleagues whose work could not be cited due to space restrictions. JA partially was supported by Gerencia Regional de Salud (Junta de Castilla y León), GRS 1342 / A / 16.

REFERENCES

1. Motley R, Kersey P, Lawrence C. Multiprofessional guidelines for the management of the patient with primary cutaneous squamous cell carcinoma. Br J Dermatol. 2002; 146:18–25. [PubMed: 11841362]
2. Preston DS, Stern RS. Nonmelanoma cancers of the skin. N Engl J Med. 1992; 327:1649–1662. [PubMed: 1435901]
3. Karia PS, Han J, Schmults CD. Cutaneous squamous cell carcinoma: estimated incidence of disease, nodal metastasis, and deaths from disease in the United States, 2012. J Am Acad Dermatol. 2013; 68:957–966. [PubMed: 23375456]

4. Housman TS, Feldman SR, Williford PM, et al. Skin cancer is among the most costly of all cancers to treat for the Medicare population. J Am Acad Dermatol. 2003; 48:425–429. [PubMed: 12637924]
5. Miller DL, Weinstock MA. Nonmelanoma skin cancer in the United States: incidence. J Am Acad Dermatol. 1994; 30:774–778. [PubMed: 8176018]
6. Leiter U, Garbe C. Epidemiology of melanoma and nonmelanoma skin cancer--the role of sunlight. Adv Exp Med Biol. 2008; 624:89–103. [PubMed: 18348450]
7. Calin GA, Sevignani C, Dumitru CD, et al. Human microRNA genes are frequently located at fragile sites and genomic regions involved in cancers. Proc Natl Acad Sci U S A. 2004; 101:2999–3004. [PubMed: 14973191]
8. Iorio MV, Croce CM. MicroRNA dysregulation in cancer: diagnostics, monitoring and therapeutics. A comprehensive review. EMBO Mol Med. 2012; 4:143–159. [PubMed: 22351564]
9. Lu J, Getz G, Miska EA, et al. MicroRNA expression profiles classify human cancers. Nature. 2005; 435:834–838. [PubMed: 15944708]
10. Volinia S, Calin GA, Liu CG, et al. A microRNA expression signature of human solid tumors defines cancer gene targets. Proc Natl Acad Sci U S A. 2006; 103:2257–2261. [PubMed: 16461460]
11. O'Day E, Lal A. MicroRNAs and their target gene networks in breast cancer. Breast Cancer Res. 2010; 12:201. [PubMed: 20346098]
12. Wang A, Landen NX, Meisgen F, et al. MicroRNA-31 is overexpressed in cutaneous squamous cell carcinoma and regulates cell motility and colony formation ability of tumor cells. PLoS One. 2014; 9:e103206. [PubMed: 25068518]
13. Xu N, Zhang L, Meisgen F, et al. MicroRNA-125b down-regulates matrix metallopeptidase 13 and inhibits cutaneous squamous cell carcinoma cell proliferation, migration, and invasion. J Biol Chem. 2012; 287:29899–29908. [PubMed: 22782903]
14. Sonkoly E, Loven J, Xu N, et al. MicroRNA-203 functions as a tumor suppressor in basal cell carcinoma. Oncogenesis. 2012; 1:e3. [PubMed: 23552555]
15. Bruegger C, Kempf W, Spoerri I, et al. MicroRNA expression differs in cutaneous squamous cell carcinomas and healthy skin of immunocompetent individuals. Exp Dermatol. 2013; 22:426–428. [PubMed: 23711067]
16. Dziunycz P, Iotzova-Weiss G, Eloranta JJ, et al. Squamous cell carcinoma of the skin shows a distinct microRNA profile modulated by UV radiation. J Invest Dermatol. 2010; 130:2686–2689. [PubMed: 20574436]
17. Navarro P, Gomez M, Pizarro A, et al. A role for the E-cadherin cell-cell adhesion molecule during tumor progression of mouse epidermal carcinogenesis. J Cell Biol. 1991; 115:517–533. [PubMed: 1918152]
18. Linardopoulos S, Street AJ, Quelle DE, et al. Deletion and altered regulation of p16INK4a and p15INK4b in undifferentiated mouse skin tumors. Cancer Res. 1995; 55:5168–5172. [PubMed: 7585567]
19. Oft M, Akhurst RJ, Balmain A. Metastasis is driven by sequential elevation of H-ras and Smad2 levels. Nat Cell Biol. 2002; 4:487–494. [PubMed: 12105419]
20. Wong CE, Yu JS, Quigley DA, et al. Inflammation and Hras signaling control epithelial-mesenchymal transition during skin tumor progression. Genes Dev. 2013; 27:670–682. [PubMed: 23512660]
21. Lena AM, Shalom-Feuerstein R, Rivetti di Val Cervo P, et al. miR-203 represses 'stemness' by repressing DeltaNp63. Cell Death Differ. 2008; 15:1187–1195. [PubMed: 18483491]
22. Tran MN, Choi W, Wszolek MF, et al. The p63 protein isoform DeltaNp63alpha inhibits epithelial-mesenchymal transition in human bladder cancer cells: role of MIR-205. J Biol Chem. 2012; 288:3275–3288. [PubMed: 23239884]
23. Yi R, Poy MN, Stoffel M, et al. A skin microRNA promotes differentiation by repressing 'stemness'. Nature. 2008; 452:225–229. [PubMed: 18311128]
24. Taube JH, Malouf GG, Lu E, et al. Epigenetic silencing of microRNA-203 is required for EMT and cancer stem cell properties. Sci Rep. 2013; 3:2687. [PubMed: 24045437]

25. Nissan X, Denis JA, Saidani M, et al. miR-203 modulates epithelial differentiation of human embryonic stem cells towards epidermal stratification. Dev Biol. 2011; 356:506–515. [PubMed: 21684271]
26. Gastaldi C, Bertero T, Xu N, et al. miR-193b/365a cluster controls progression of epidermal squamous cell carcinoma. Carcinogenesis. 2014; 35:1110–1120. [PubMed: 24374827]
27. Viticchie G, Lena AM, Cianfarani F, et al. MicroRNA-203 contributes to skin re-epithelialization. Cell Death Dis. 2012; 3:e435. [PubMed: 23190607]
28. Gubian S SAaSP. ExiMiR: R functions for the normalization of Exiqon miRNA array data. R package version 2.10.0. 2012.
29. R-Development-Core-Team. R Foundation for Statistical Computing. Vienna, Austria: 2010. A language and environment for statistical computing.
30. Irizarry RA, Hobbs B, Collin F, et al. Exploration, normalization, and summaries of high density oligonucleotide array probe level data. Biostatistics. 2003; 4:249–264. [PubMed: 12925520]
31. Demey JR, Vicente-Villardon JL, Galindo-Villardon MP, et al. Identifying molecular markers associated with classification of genotypes by External Logistic Biplots. Bioinformatics. 2008; 24:2832–2838. [PubMed: 18974073]
32. Brantsch KD, Meisner C, Schonfisch B, et al. Analysis of risk factors determining prognosis of cutaneous squamous-cell carcinoma: a prospective study. Lancet Oncol. 2008; 9:713–720. [PubMed: 18617440]
33. Karia PS, Jambusaria-Pahlajani A, Harrington DP, et al. Evaluation of American Joint Committee on Cancer, International Union Against Cancer, and Brigham and Women's Hospital tumor staging for cutaneous squamous cell carcinoma. J Clin Oncol. 2013; 32:327–334. [PubMed: 24366933]
34. Cherpelis BS, Marcusen C, Lang PG. Prognostic factors for metastasis in squamous cell carcinoma of the skin. Dermatol Surg. 2002; 28:268–273. [PubMed: 11896781]
35. Di Leva G, Garofalo M, Croce CM. MicroRNAs in cancer. Annu Rev Pathol. 2013; 9:287–314. [PubMed: 24079833]
36. Hayes J, Peruzzi PP, Lawler S. MicroRNAs in cancer: biomarkers, functions and therapy. Trends Mol Med. 2014; 20:460–469. [PubMed: 25027972]
37. Yu J, Peng H, Ruan Q, et al. MicroRNA-205 promotes keratinocyte migration via the lipid phosphatase SHIP2. FASEB J. 2010; 24:3950–3959. [PubMed: 20530248]
38. Wang N, Li Q, Feng NH, et al. miR-205 is frequently downregulated in prostate cancer and acts as a tumor suppressor by inhibiting tumor growth. Asian J Androl. 2013; 15:735–741. [PubMed: 23974361]
39. Gregory PA, Bracken CP, Bert AG, et al. MicroRNAs as regulators of epithelial-mesenchymal transition. Cell Cycle. 2008; 7:3112–3118. [PubMed: 18927505]
40. Wei T, Orfanidis K, Xu N, et al. The expression of microRNA-203 during human skin morphogenesis. Exp Dermatol. 2010; 19:854–856. [PubMed: 20698882]
41. Wang D, Zhang Z, O'Loughlin E, et al. MicroRNA-205 controls neonatal expansion of skin stem cells by modulating the PI(3)K pathway. Nat Cell Biol. 2013; 15:1153–1163. [PubMed: 23974039]
42. Frierson HF Jr, Cooper PH. Prognostic factors in squamous cell carcinoma of the lower lip. Hum Pathol. 1986; 17:346–354. [PubMed: 3957335]
43. Veness MJ. High-risk cutaneous squamous cell carcinoma of the head and neck. J Biomed Biotechnol. 2007; 2007:80572. [PubMed: 17541471]
44. Tarin D, Thompson EW, Newgreen DF. The fallacy of epithelial mesenchymal transition in neoplasia. Cancer Res. 2005; 65:5996–6000. discussion-1. [PubMed: 16024596]
45. Garber K. Epithelial-to-mesenchymal transition is important to metastasis, but questions remain. J Natl Cancer Inst. 2008; 100:232–233. 9. [PubMed: 18270330]
46. Ledford H. Cancer theory faces doubts. Nature. 2011; 472:273. [PubMed: 21512545]
47. Cai J, Fang L, Huang Y, et al. miR-205 targets PTEN and PHLPP2 to augment AKT signaling and drive malignant phenotypes in non-small cell lung cancer. Cancer Res. 2013; 73:5402–5415. [PubMed: 23856247]

48. Lei L, Huang Y, Gong W. miR-205 promotes the growth, metastasis and chemoresistance of NSCLC cells by targeting PTEN. Oncol Rep. 2013; 30:2897–2902. [PubMed: 24084898]

49. Qu C, Liang Z, Huang J, et al. MiR-205 determines the radioresistance of human nasopharyngeal carcinoma by directly targeting PTEN. Cell Cycle. 2012; 11

50. Gandellini P, Folini M, Longoni N, et al. miR-205 Exerts tumor-suppressive functions in human prostate through down-regulation of protein kinase Cepsilon. Cancer Res. 2009; 69:2287–2295. [PubMed: 19244118]

51. Tucci P, Agostini M, Grespi F, et al. Loss of p63 and its microRNA-205 target results in enhanced cell migration and metastasis in prostate cancer. Proc Natl Acad Sci U S A. 2012; 109:15312–15317. [PubMed: 22949650]

52. Barrette K, Van Kelst S, Wouters J, et al. Epithelial-Mesenchymal Transition during invasion of cutaneous Squamous Cell Carcinoma is paralleled by AKT activation. Br J Dermatol. 2014

ABBREVIATIONS

CSCC	Cutaneous Skin Cell Carcinoma
miR	miRNA

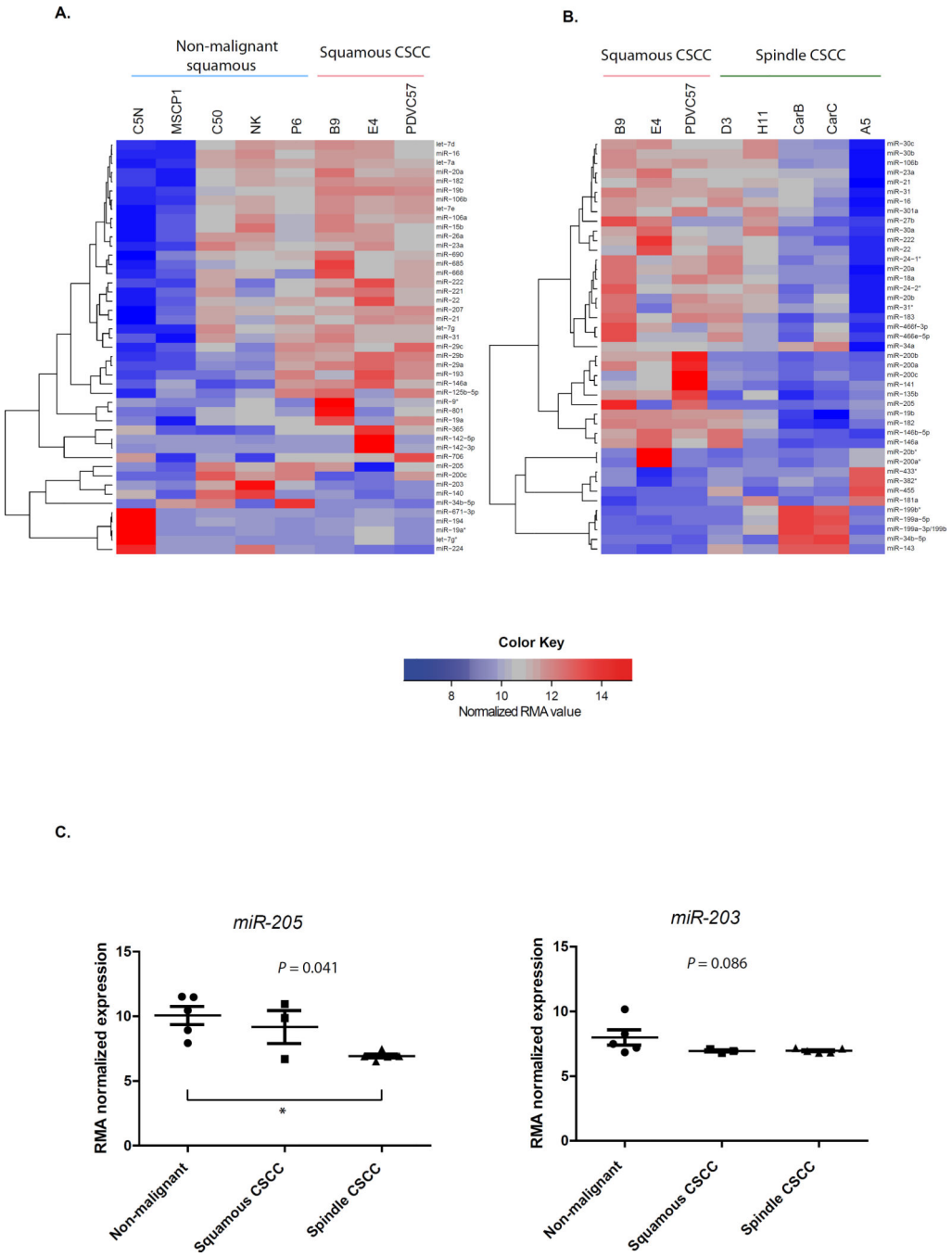

Figure 1. Expression patterns of miRNAs in murine skin cancer cell lines with different grade of aggressiveness

A) The heatmap shows the 45 miRNAs most differentially expressed between CSCC cell lines (PCVC57, B9, E4) and non-malignant skin cell lines, which included immortalized keratinocytes (C50, C5N, NK) and cells from benign papillomas (MSCP1, P6) generated by the DMBA/TPA protocol of carcinogenesis. **B**) Heatmap showing the 43 miRNAs most differentially expressed between squamous CSCC cell lines (PCVC57, B9, E4) and the spindle group of CSCC cell lines (H11, A5, D3, CarB, CarC), that presented an EMT

process. The lists of miRNAs from A and B heatmaps are shown in Supplementary Tables S3A and S3B, respectively. The A5 cell line was analysed from two different clones as an internal assay control and, as expected, both samples clustered together. In A and B, quantile normalization was performed using the Robust Microarray Analysis (RMA) algorithm, as indicated in the scale of the figure and in the material and methods section. **C**) Expression of the *miR-205* (left) and the *miR-203 (right)* in the different groups of skin cell lines. The *P*-value indicated was obtained by the Kruskal-Wallis test. The asterisk indicates in between which groups there is statistical significance after applying the Dunn's multiple comparison test.

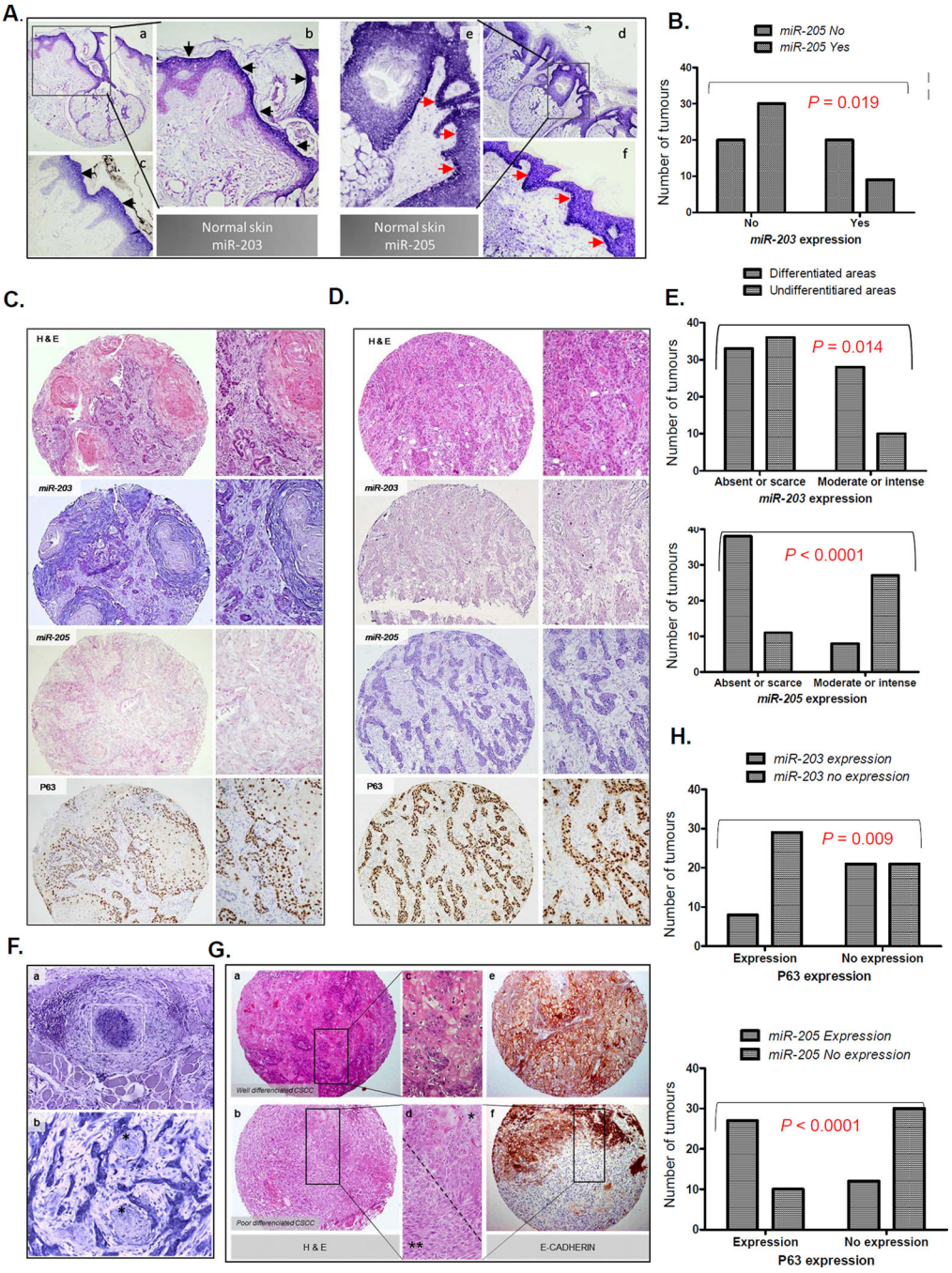

Figure 2. Expression of *miR-203* and *miR-205* in human CSCC

A) Expression of *miR-203* and *miR-205* in normal skin as determined by *in situ* hybridization (ISH). Markedly, *miR-203* is expressed in the epidermal upper layers of the epidermis (a, b (100x) and c (400x), black arrowheads), whereas *miR-205* is expressed in the basal and immediately suprabasal layers of the epithelia (d, e (100x) and f (400x), red arrowheads). **B**) Mutually exclusive expression of miR-205 and miR-203 in CSCC. Pearson's Chi-square test. **C**) Example of a well-differentiated CSCC. The haematoxylin and eosin (H&E) section shows intense keratinization in the central zones of the tumoural

lobules (100x and 400x). The pictures show *miR-203* and *miR205* expression by ISH and P63 expression by immunohistochemistry (IQ) from the same tumour, as indicated in the pictures. *MiR-203* is highly expressed, whereas *miR-205* and P63 were poorly expressed. **D**) Example of a poorly-differentiated CSCC. The H&E section shows strands of epithelial cells without keratinization (100x). *MiR-205* and P63 were highly expressed, whereas *miR-203* is poorly expressed. In C and D, pictures on the right correspond to more augmented details (400x) from the ones on the left (100x). **E**) Quantification of *miR-203* and *miR-205* expression in differentiated and undifferentiated areas of CSCC. Pearson's Chi-square test. **F**) Upper figure: Strong *miR-205* expression in CSCC cells that are forming an intravascular tumoural thrombus (a, and white square) (400x). Lower figure: High *miR-205* expression present in tumoral cells in the front of invasion with perineural infiltration (b) (400x). Nerves are indicated by an asterisk (⁎). **G**) H&E staining (a,b,c,d) and E-CADHERIN expression (e, f) (100x) done by immunohistochemistry in a well- (a,d,e) and poorly-differentiated (b,d,f) CSCCs. There is strong E-CADHERIN expression in the epithelial cells of the well-differentiated CSCC (e) (100x). In d (400x), there are typical epithelial cells in the upper portion of the picture (⁎) that correspond to zones with strong staining to E-CADHERIN (f, upper portion of the spot), and tumoral spindle cells in the lower one (⁎ ⁎) that correspond to zones without expression of E-CADHERIN (f, lower portion of the spot). This zone illustrates the tumour heterogeneity and the epithelial to mesenchymal transition process. **H**) Upper figure: *miR-203* expression is significantly absent when P63 is present. Lower figure: *miR-205* and P63 coexpressed in the same tumours in a statistically significant manner. *P* values were obtained by the Pearson's Chi-square test.

Table 1

Associations of poor clinical evolution of CSCCs with

A) histopathological tumor features, and **B**) *miR-205* and *mi-R203* expression. N.S. not significant. Red: significant *P* values. Blue: statistical trend.

			POOR PROGNOSIS CRITERIA								
			Local Recurrence			Nodal Progression			Events of Poor Clinical Evolution		
			YES	NO	*P*-value	YES	NO	*P*-value	YES	NO	*P*-value
A. Pathological Tumour Traits	Growth Pattern	Expansive	0	26		1	15		1	25	
		Mixed	1	16	N.S.	1	16	0.064	2	15	0.066
		Infiltrative	3	33		8	28		9	27	
	Grade of Differentiation	Good	1	24		1	24		2	23	N.S.
		Moderate	2	35	N.S.	3	34	0.006	5	32	
		Poor	1	16		6	11		5	12	
	Perineural Invasion	YES	3	11		4	10		5	9	
					0.002			0.048			0.018
		NO	1	64		6	59		7	58	
	Desmoplasia	YES	2	19		3	18		3	18	
					N.S.			N.S.			N.S.
		NO	2	56		7	51		9	49	
	Tumour Thickness	(Median in mm (SD))	11.5(14.5)	5.28(4.5)	0.009	6.25(5.25)	5(4.50)	0.035	8 (7.75	5 (4.58)	0.003
	Tumour Size	(Median in mm (SD))	21.5(44.5)	18(9)	N.S.	22(10.25)	18(8)	N.S.	22(10)	18(9)	0.074
B. mIRNAs expression	*miR-203*	Expression	0	29		2	27		2	27	
					N.S.			N.S.			N.S.
		No expression	4	46		27	42		10	40	
	miR-205	Expression	4	35		7	32		10	29	
					0.038			N.S.			0.011
		No expression	35	40		3	37		2	38	

Table 2

Definition of CSCC prognosis by multivativariate analyses

A) Pathological features of CSCC associated with a poor clinical evolution obtained by logistic regression. **B**) Characteristics of the three clusters of CSCCs identified by the logistic biplot. The table shows the number and percentage of tumours within each cluster that showed the characteristics indicated.

A. Logistic regression models of prognosis					
		Variables	**OR**	**CI 95%**	***P* value**
Local Recurrence		Perineural infiltration	17.445	1.662–183.359	0.017
Nodal Progression		Grade of differentiation	7.909	1.912–32.717	0.004
Events of Poor Clinical Evolution		*miR-205* expression	6.552	1.332–32.232	0.021
B. Clusters of prognosis identified by logistic biplot					
		Cluster 1 N=25(31.6%)	**Cluster 2 N=31 (39.2%)**	**Cluster 3 N=23 (29.1%)**	***P* value**
Events of Poor Clinical Evolution		1 (4%)	3 (9.7%)	8 (34.8%)	0.007
miRNAs expression	***miRNA-203***	15 (60%)	11 (35.5%)	3 (13%)	0.007
	miRNA-205	3 (12%)	15 (48.4%)	21 (91.3%)	0.0001
Pathological Tumour Traits	**Infiltrative Growth Pattern**	12 (48%)	4 (12.9%)	22 (95.7%)	0.002
	Poor Grade of Differentiation	2 (8%)	25 (80.6%)	13 (56.5%)	0.043
	Perineural Infiltration	1 (4%)	0	13(56.5%)	0.0001
	Desmoplasia	1 (4%)	0	13(56.5%)	0.0001